

Smart films of carbohydrate-based/sunflower wax/purple Chinese cabbage anthocyanins: A biomarker of chicken freshness

Sulafa B.H. Hashim^{a,b}, Haroon Elrasheid Tahir^a, Li Lui^a, Junjun Zhang^a, Xiaodong Zhai^a, Amer Ali Mahdi^a, Nosyba A. Ibrahim^b, Gustav Komla Mahunu^c, Mahmoud M. Hassan^b, Zou Xiaobo^a, Shi Jiyong^{a,*}

^a School of Food and Biological Engineering, Jiangsu University, 301 Xuefu Rd., 212013 Zhenjiang, Jiangsu, China

^b Department of Food Technology, Faculty of Agricultural Technology and Fish Sciences, Alneelain University, Khartoum, Sudan

^c Department of Food Science & Technology, Faculty of Agriculture, Food and Consumer Sciences, University for Development Studies, Tamale, Ghana

ARTICLE INFO

Keywords:

pH-colorimetric sensor film
Sunflower wax
Agar and methylcellulose matrix
Purple Chinese cabbage
Biomarker
Chicken breast freshness

ABSTRACT

Innovative pH-colorimetric sensor film was fabricated from agar and methylcellulose matrix (AM) with various concentrations of sunflower wax (SFW) (6%, 9%, 12%, and 15% w/w) combined with purple Chinese cabbage (CPC) anthocyanins for tracking chicken breast freshness. A bio-composition film AM/CPC with (hydrophobic) SFW exhibited significant color variations in acidic pH level of (2–6) and a slight shift in alkaline pH levels ranging from (7–12), as well as marked color change due to ammonia vapor. Microstructure analyses revealed that SFW was fixed effectively into the AM-CPC matrices. The incorporation of varying SFW concentrations enhanced the mechanical, thermal, antioxidant activity, reduced anthocyanin release and physical properties (mainly water vapor permeability), with the best performance at AM/CPC/9% SFW. Interestingly, SFW films demonstrated perfect defense opposing UV-vis and visible light. Finally, it was proved that the efficiency of the pH-colorimetric film as an indicator for evaluating the freshness of chicken breast.

1. Introduction

Smart packaging is a modern transformation in packaging technologies, especially in the food sector. It can provide multiple functions in real-time and improve the present food quality, freshness, and/or safety level. Furthermore, it is determined by monitoring the food change inside packaging by sensing, detecting, and giving information to processors and consumers about the food quality status, leading to less waste and hazardous food (Kalpana et al., 2019). Smart sensors and labels can be attached to packaging for measuring the progression of biological media as a biochemical indicator or biomarker like TVB-N to monitor meat freshness (Azarifar and Ghanbarzadeh, 2020).

A recent study shows that anthocyanins are among the most biologically active compounds receiving significant attention in the food industry due to their high antioxidants which promote human health (Khoo et al., 2017). Most anthocyanins categories (such as cyanidin, delphinidin, pelargonidin, peonidin, petunidin, and malvidin) are able to isomerize and donor electron hydroxyl group conversions in various pH solutions utilizing a wide range of colors, and potentially operating

as pH sensors (Bhargava et al., 2020; de Oliveira Filho et al., 2021). Furthermore, Bhargava et al. (2020) asserted that anthocyanins are extraordinarily reactive, potentially serving as indicators of food quality, particularly for their pH colorimetric attributes in the food packaging materials.

The Purple Chinese Cabbage (*Brassica rapa L. ssp. pekinensis*), is a dietary vegetable crop native to China, and is widely cultivated as an economic plant in Asian countries. It is colorful, nutritious, and source of anthocyanins. Additionally, the purple Chinese cabbage has four types of anthocyanins (cyanidin, delphinidins, peonidin, and petunidin) that make up over 70 % of its composition (He et al., 2016).

Solid package matrices (biodegradable, safe, and comprised sensors) are used to create new smart food packaging materials. A series of innovative pH colorimetric sensor materials were integrated into the biopolymers as food quality indicators utilizing colorimetric pigment shifts such as anthocyanin and curcumin due to reactions with the package environment's pH change, which are observable through colorimetric changes by the naked eye. In this scenario, the color change could be indicative of food spoilage. These colorimetric biopolymer

* Corresponding author.

E-mail address: shi_jiyong@ujs.edu.cn (S. Jiyong).

<https://doi.org/10.1016/j.foodchem.2022.133824>

Received 9 January 2022; Received in revised form 27 July 2022; Accepted 27 July 2022

Available online 29 July 2022

0308-8146/© 2022 Elsevier Ltd. All rights reserved.

films require more durability by improving the mechanical properties and protecting sensor materials from ultraviolet light and oxidation, reducing their susceptibility to moisture from the environment or food within the package, especially natural pigments and most polysaccharides (hydrophilic substances).

Agar is a polysaccharide synthesized from red algae of the Rhodophyceae class. However, agar film is limited in the food packaging sector due to its highly hydrophilic and poor mechanical, optical, and thermal properties (Mostafavi & Zaeim, 2020). Methylcellulose is a cellulose derivative utilized in a wide range of industrial food products (Nasatto et al., 2015). Nevertheless, moisture vapor from the food within the container weakens the film's mechanical properties and its resistance to VWP (Alizadeh-Sani et al., 2021; Halim et al., 2018). Therefore, many materials, such as lipids (which have long fatty acids such as natural waxes) can be used to overcome these problems (Hashim et al., 2022; Dos Santos et al., 2017; Syahida et al., 2020; Cortés-Rodríguez et al., 2020), which exhibit high hydrophobicity to enhance all prospective characteristics (moisture, light, thermal, and mechanical properties) of films.

Sunflower wax (SFW) could also be a good candidate for utilization as an improvement agent within agar and methylcellulose film. It is one of the by-products of the sunflower oil industry and is marked by its availability and lower price. In general, SFW has a melting point of 76.82 ± 0.13 °C and long-chain fatty esters (C₃₈–C₅₄) (Goslińska & Heinrich, 2019). Many previous studies (Baümler et al., 2013; Yilmaz et al., 2021) report on the advantageous ability of SFW to be used in food sectors. SFW is a low-cost by-product that is also an eco-friendly biomaterial. SFW could be employed as an alternative to synthetic petroleum wax hydrophobic compounds used in food packaging to improve overall properties, particularly in a colorimetric film containing anthocyanin. By integrating them into intelligent packaging, non-polar compounds could be used to overcome the problem of reducing anthocyanin sensitivity to leach in polar biomaterial matrixes.

Unfortunately, no research has been done on the use of SFW in colorimetric films to boost packaging film hydrophobicity. Furthermore, to the best of our knowledge, SFW and anthocyanins from purple Chinese cabbage (CPC) are developed in an Agar-Methylcellulose (AM) matrix as a colorimetric film sensitive to food spoilage biomarkers in food packaging has not been recorded yet. As such, improving the properties (optical, mechanical, thermal, release, and antioxidant) of the AM (carbohydrate, hydrophilic) colorimetric films was one of the goals of developing the freshness films employing various concentrations of SFW (lipid, hydrophobic). Finally, the developed film was utilized to determine the freshness of chicken breasts stored at 25 °C.

2. Materials and experiments

2.1. Materials

SFW was bought from Union Chemical IND. (Shanghai) CO., Ltd. Agar, Methylcellulose, Tween 80, DPPH radical scavenging, and lecithin were purchased from Sinopharm Chemical Reagent Co., Ltd. (Shanghai, China). Purple Chinese cabbage and chicken breast were bought from a Zhenjiang market in Jiangsu province (China). Ammonia hydroxide (25 %–28 %), glycerin, acetic acid, methanol, and ethanol were purchased from Shanghai Natural Wild-insect Kingdom Co. Ltd. Citric acid, disodium citrate, and Disodium hydrogen phosphate were provided by Jiangsu Thorpe Group Co., Ltd.

2.2. Extraction of purple Chinese cabbage (CPC) anthocyanins

The CPC was cut into small pieces, dehydrated for 24 h in an oven at 45 °C, and crushed to a powder of about 50 g, which was then mixed with ethanol 75 % in 1:20 (w/v) ratio, then stirred in a water bath at 45 °C for 6 h before being filtrated (Whatman paper No.1). After that, the mixture was centrifuged to remove non-dissolving residues at 3500

rpm for 12 min and concentrated at 45 °C through use of an evaporator contained in a vacuum. The anthocyanin content of CPC extract was measured on bases (cyanidin-3-glucoside) by the previously described method with slight modifications (Kanatt, 2020). The estimated anthocyanin content was 69.17 ± 0.757 mg/g.

2.3. Identification of anthocyanins in CPC extraction by HPLC–MS (High-performance liquid chromatography-mass spectrometer)

A CPC crude anthocyanin extraction was purified using the Sep-Pak C18 cartridge (Long Body Sep-Pak Plus; Waters Associates, Milford, MA). A qualitative analysis of purified CPC was then performed by HPLC-MS with a Thermo Electron Surveyor MS pump and a surveyor autosampler injector (Thermo Electron, San Jose, CA) connected to a ZORBAX SB-C18 column (lichrospher5-C18, 150 mm, 4.6 mm, 5 µm, Agilent Technologies, Santa Clara, CA). The temperature of the column oven was fixed at 35 °C, the wavelength was adjusted at 530 nm, with an injection volume (7 µL) and flow rate of 0.5 mL/min; and the capillary voltage was 3 kV for a positive (ESI +) mode and a scan range of 50–2000 Da was set. The mixture solvent system of (A) 0.1 % formic acid solution and (B) acetonitrile was rectified as follows: 10 %–30 %B; 0–15 min, 10–30 % B; 15–25 min, 30–50 % B; 25–30 min, 50–30 % B; 30–35 min, 30–10 % B; 35.01 min, 10 % B.

2.4. UV–Vis spectra of CPC at different pH (2–12)

UV–Vis spectra of the CPC anthocyanin extract of color change were obtained utilizing a UV–Vis spectrophotometer (Agilent CARY 100, Varian Corporation, USA) at various pH values ranging from 2.0 to 12.0 at wavelength ranges of 400–700 nm.

2.5. Development of colorimetric films

Agar-Methylcellulose (AM) emulsion was made from 2 g of agar and 1 g of methylcellulose dissolved in distilled water (100 mL) with glycerol (2 g) and blended in a magnetic stirrer (F–101S, YUHUA, China) for 2 h at 95 °C. The SFW emulsion was made according to the previous method (Hashim et al., 2022) with some modifications. Concisely, SFW granular (4 g) was dissolved in ethanol (100 mL, 95 %) in a water bath and stirred continuously at 85 °C for 1 h. Then, soy lecithin and Tween 80 were added at ratios of (5 % and 20 % w/w) of the SFW and stirred for 20 min at 80 °C. The hydrophilic (AM) emulsion was mixed with the (SFW) hydrophobic emulsion at various concentrations (6 %, 9 %, 12 %, and 15 % w/w of AM) for 30 min at 80 °C. From there, the mixture temperature was lowered to 65 °C, and 0.7 g/100 mL of CPC anthocyanins powder dye was added using steady stirring for 30 min, followed by ultrasonication (Branson CPX5800H, USA) at 65 °C for 5 min to remove the trapped bubbles. Then, 95 g of the individual film emulsion was transferred to (23 cm x16.5 cm) plates and dried at 30 °C for 24 h. Lastly, dehydrated films were stored in the dark at room temperature and humidity of 50 ± 5 % for further examination. As such, the five films were coded in the following order: AM/CPC as the control film, AM/CPC/6% SFW, AM/CPC/9%SFW, AM/CPC/12 %SFW, and AM/CPC/15 %SFW.

2.6. Morphology of the colorimetric films

2.6.1. Fourier transforms infrared (FTIR)

Fourier transforms infrared spectra of the film samples were obtained using a Nicolet 50 FTIR spectrophotometer (ThermoFisher, USA) in the range of $4000\text{--}400$ cm⁻¹ with a resolution of 65 scans at 0.005 cm⁻¹.

2.6.2. Scanning electron microscopy (SEM)

The film morphology of the surface was measured with SEM (S-4800, Hitachi High Technologies Corporation, Japan). First, the colorimetric films were dehydrated at 35 °C for 2 h and fixed onto the aluminium

tape stubs, and then sputtered with gold spraying coated under vacuum at an accelerated voltage of 15 kV.

2.6.3. X-ray diffraction analysis

The XRD diffraction spectra of films and biomaterial were assessed by X-ray diffractometer (Bruker, D8 ADVANCE, Germany) of Cu K α as reference point radiation, with a voltage of 40 kV, a current of 30 mA, a scanning rate of 2°(2 θ)/min, at 5° to 50° (2 θ) an angle range.

2.7. Mechanical properties

The film thickness was randomly estimated with an electronic micrometer (Sanfeng Group Co., China) at 6 different points. The tensile strength (TS, MPa), and elongation at break (EB, %) properties of the film samples (6 cm \times 2 cm) were measured by an electronic texture analyzer testing machine (Instron Corporation, TA-XT2i, USA) at a crossheading rate of 0.6 mm/s. The prime grip intensity was immovable at 30 mm with 50 kg (490.3325 N) of a weight cell according to Eqs. (1) and (2) respectively.

$$TS \text{ (MPa)} = F/A \quad (1)$$

$$EB \text{ (%) } = \Delta L/L_0 \times 100 \quad (2)$$

where F is maximum stretching strength (N); A is the surface area of films (cm²); ΔL and L_0 are elongated and original lengths (cm) of film samples, respectively.

2.8. Moisture barrier properties of colorimetric films

2.8.1. Moisture content (MC), water solubility (WS), and Swelling capacity (S)

The MC, WS, and S percentages were measured, as described in our previous work (Hashim et al. 2022).

2.8.2. Water vapor permeability (WVP)

WVP of films was evaluated as mentioned by Alizadeh et al. (2021) with some modifications. The colorimetric films (28 mm, diameter) were initially covered in beakers containing deionized water (10 mL) and held at the 25 % RH and 25 °C in the desiccator chamber. Therefore, the absorbed vapor on films was estimated by the beaker weight change regularly for 5 days and calculated using Eq. (3):

$$WVP = (\Delta w \times L) / \Delta p \times S \times t \quad (3)$$

where WVP is water vapor permeability (gm⁻² d⁻¹); Δw is the film samples weight change (g); S is the film area (mm²); L is the thickness (mm, an average of 6 points taken on the film); t is time per day, and Δp is the vapor pressure difference of film (1583.7 Pa at 25 °C).

2.9. Anthocyanin release from the colorimetric films

A release test was determined to examine the stability of CPC anthocyanin in the films, according to (Liang et al., 2019), with some modifications. The colorimetric films (0.04 g) were immersed in 10 mL of mimetic model foodstuffs (50 % and 95 %) ethanol solution for 10 h at 100 rpm and 25 °C. After that, the films were removed, and the spectra of the residue solutions were reported in the range of 475 to 800 nm using a UV-vis spectrophotometer (Agilent CARY 100, USA).

2.10. Light transmittance of colorimetric films

A spectrophotometer UV-Vis was assessed at 200 to 800 nm of the transparency spectra of films (1 cm \times 2 cm) according to the procedure described by Hashim et al. (2022).

2.11. Thermal stability of colorimetric films

The blend films' thermogravimetric analysis (TGA/DTG) were recorded using a thermogravimetric analyzer (NETZSCH STA 449F3 model). The films (10 mg) were placed in a standard aluminium pan and heated from 30 °C to 600 °C at a heating rate of 10 °C/min under a 50 cm³/min nitrogen flow, and changes in their mass with temperature were measured.

2.12. Antioxidant activity of colorimetric films

The antioxidant activity was estimated using a slight modification to determine the DPPH radical scavenging activity following Wu et al. (2021). Firstly, the film strip weight (20 mg) was dipped in DPPH solution in methanol (4 mL, 0.25 μ M) and kept in the dark at 20 °C for 1 h. Secondly, 3 mL of the sample supernatant was evaluated at 517 nm by a spectrophotometer, and the DPPH scavenging rate was calculated.

2.13. Color stability of colorimetric films

The stability of the CPC anthocyanin pigments in the various films was measured with a moveable colorimeter (PSC-30, EVERFINE; China). The colorimetric films were kept at 4 °C and 25 °C with 50 % RH. According to Eq. (4), the total number of color difference (ΔE) values were calculated daily for 16 days.

$$\Delta E = \sqrt{(L_s - L_0)^2 + (a_s - a_0)^2 + (b_s - b_0)^2} \quad (4)$$

where; L_0 (the lightness), a_0 (red to green), and b_0 (yellow to blue) are the primary grey values; L_s , a_s , and b_s are the colors after storage.

2.14. Color reaction to pH and ammonia of colorimetric films

The response of colorimetric film to pH solutions of 2.0 to 12.0 with immersed (1 cm x1 cm) film for 2 min, producing an image captured on an optical scanner device (G4050Scanjet, HP). The films' reactions with volatile ammonia concentration (100 mmol/L) were estimated via a chromatic scanner (G4050Scanjet, HP). The films (2 cm \times 2 cm) were wrapped on the upper test tubes containing ammonia water (10 mL) for 0, 10, 20, 30, and 40 min to sense the color change. The RGB values representing films were evaluated in the Matlab R2012a program (Matworks Inc., Natick, MA, USA). Finally, the colorimetric film performed with ammonia sensitivity (S_{RGB}) was then evaluated according to Eq. (5):

$$S_{RGB} = \frac{|R_a - R_b| + |G_a - G_b| + |B_a - B_b|}{R_a + G_a + B_a} \times 100 \quad (5)$$

R_a , G_a , and B_a are red, green, and blue; R_b , G_b , and B_b are the values after storage.

3. The chicken breast spoilage

3.1. Film color change (ΔE)

All five films were used to observe the ability to display the freshness of chicken breast. The films (2 cm \times 2 cm) were placed in the headspace of the top box of packaging containing 200 g of fresh chicken breast (4 cm, height from the chicken) at a storage temperature of 25 °C. Film color transformation values were scanned with a movable chromameter (KONICA MINOLTA, CR-400, Japan) every 3 h for 42 h.

3.1.1. Determination of the total volatile basic nitrogen (TVB-N)

TVB-N concentrations in the chicken breast were measured during the storage according to the Chinese standard method (GB 5009.228-2016). Briefly, the chicken breast samples were minced and

homogenized by a homogenizer (A-88, Jintan medical instrument factory, Jiangsu, China). Then, 10 g of the minced-homogenized samples were blended with 75 mL of deionized water. After that, the mixture was thoroughly mixed by shaking for 30 min and then transferred to a distillation tube. Then, 1 g of magnesium oxide (MgO) was added to the distillation tube of an automatic Kjeldahl ammonia determinator (K9840, Hanon instrument, Shandong, China) then a 30 mL boric acid solution (H₃BO₃, 20 g/L) was added after that the distillation solution received within 3 min. The distillation solution was immediately titrated using an automatic titrator (T860, Hanon instrument, Jinan, China). The endpoint was set to pH 4.65, using hydrochloric acid solution (HCl, 0.1 mol/L). The testing was performed in triplicate.

3.2. Statistical analysis

The attribution of the five colorimetric films was evaluated, and the three individual trials information was confirmed as the mean \pm standard deviation. Data investigation and the analysis of variance (ANOVA) were accomplished with the Minitab (Minitab, State College, Pa.). Significant differences among investigational mean values were estimated at ($P < 0.05$).

4. Results and discussion

4.1. The characterization of anthocyanins in CPC extraction by HPLC-MS

HPLC-MS was used for analysis and identified the CPC anthocyanins extract. Many peaks were reported at 530 nm, as shown in Fig. S1. Based on the approach of MS, the CPC anthocyanin's structure is shown in Table S.1. As demonstrated in Fig. S.1, the main CPC anthocyanins constituted Cyanidin-3-sophoroside-5-glucoside, Cyanidin-3-sophoroside (ferulyl)-5-glucoside malonyl, and Delphinidin-3-glucoside (sinapyl)-5-glucoside-7-glucoside. This generated similar findings as done in a previous study by He et al. (2016).

4.2. UV-vis spectra of CPC extract in different pH solutions

We designed a smart package dependent on the changes of CPC anthocyanin color under various pH levels to detect the quality attributes of chicken breast. The CPC anthocyanin spectra of color changes in the range of pH (2–12) solutions, as shown in Fig. 1. The color of CPC anthocyanins changed from dark to light red in acid pH solutions (2–4) as a structural transformation to flavylium cation, with the highest

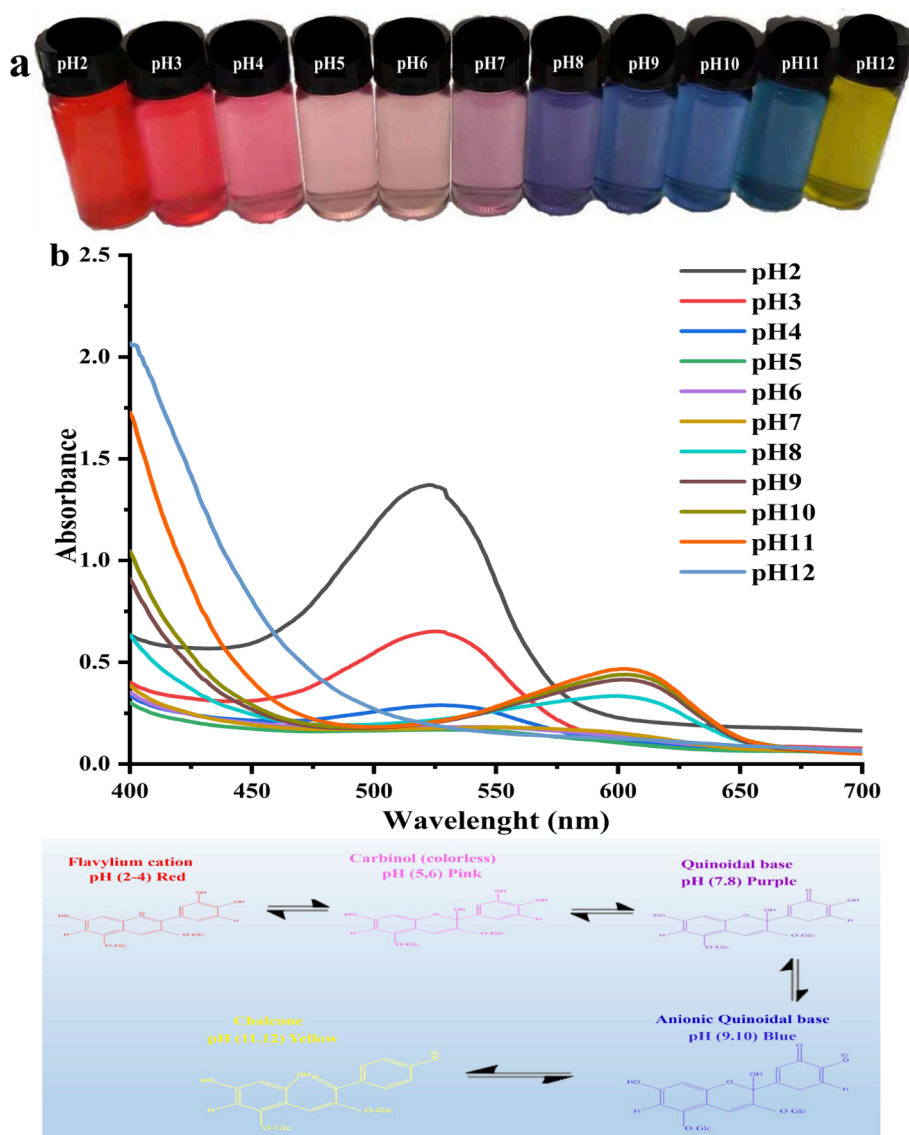


Fig. 1. (a) Colors and (b) UV-vis spectra of CPC solutions at pH 2–12.

absorption peak from 520 to 530 nm, followed by increased absorbance. At pH level of 5,6, with increased carbinol (colorless) and reactions with flavylum, the color appeared pink at 530 and 553 nm. With increases in pH neutral solution (7,8) quinoidal base was established and emitted a purple to violet color at 585 to 600 nm. As a result, at 605 nm, anion quinoidal (blue) was dominant in alkalinity pH (9–10). Interestingly, at pH (11), the color turns greenish-blue when the quinoidal base (blue) is reacted with chalcone (yellow) at 605 nm and subsequently droppings to 560 nm and turning yellow at pH (12). Similar detection has been reported for anthocyanin extracted from red barberry (Alizadeh et al., 2021) and butterfly pea flower (Hashim et al., 2022; Wu et al., 2021). The spoilage of chicken breasts can be easily detected by observing the change in the color of the smart packaging, particularly in an alkaline environment.

4.3. Morphology of colorimetric films

4.3.1. Fourier transforms infrared (FTIR)

The FTIR spectra of the agar, methylcellulose, CPC, SFW, and molecular interactions of different components of biomaterials in the five colorimetric films are revealed in Fig. 2A. The spectrum of agar showed the major absorption peaks that were positioned at 1646, 1047, 931, and 1371 cm^{-1} due to the C–N group, ester sulphate group, 3,6-anhydrogalactose, and aliphatic ether, respectively (Roy et al., 2021). The spectrum for methylcellulose showed the maximum absorption peak at 3475 cm^{-1} resulting from the (–OH) hydroxyl group band and the peaks at 1645 and 1050 cm^{-1} due to stretching of the (C=O) carbonyl and ether (C–O–C) groups (Alizadeh et al., 2021). In the CPC spectrum, the band peaks at 1623 and 1418 cm^{-1} , illustrating the (–C=C–) alkene bond of α , β -unsaturated ketone and aromatic ring phenolic of a carbonyl group. The peak at 1055 cm^{-1} was associated with an aromatic ring of C–H distortion. The CPC has a functional group similar to esters (COO), carboxylic acids, and polyphenols (Alizadeh et al., 2021; Zhai et al., 2017). The broadband at 2920 cm^{-1} and the peak at 2846 cm^{-1} in SFW spectra were designated as aliphatic (–CH) vibration groups and bend methylene. At 1736 cm^{-1} , it stretches (–C=O) functional groups of carboxylic and aldehydic acids, making them distinct from the fatty acid chain in wax (Hashim et al., 2022; Syahida et al., 2020; Y. Zhang et al., 2018). Furthermore, the bands at 1466, 1378, and 1185 cm^{-1} indicate (–CH₂), (–CH₃) bend, and (C–O) bond valence vibrations in esters, respectively. The main broadband groups that comprised molecular connections between the different constituents were stretching vibration hydroxyl groups (–OH) in the range (3360–3340 cm^{-1}) of SFW, agar, methylcellulose, CPC, and colorimetric films. Notably, the intensity areas of methylcellulose at 3475 cm^{-1} , agar at 2885 cm^{-1} and CPC at 3430 cm^{-1} shifted after the incorporation of SFW (6, 9, 12, and 15 %)

into films from 3374, 3360 to 3339 and 2929 cm^{-1} , indicating that reduced intermolecular hydrogen bonds were formed in the matrix of the film. According to previous studies conducted by Hashim et al. (2022) and Syahida et al. (2020), the film comprising of SFW at 1736 cm^{-1} relates to the C=O stretching vibrations of the ester carbonyl fatty acid molecules which were successfully incorporated into the film network.

4.3.2. Scanning electron microscopy

SEM images exposed alterations in the surface morphology of the studied films at an enlargement of 150 μm in Fig.S.2. In general, various films' surface structures were relatively smooth and homogenous. Nevertheless, SEM images show disparities between control film (AM/CPC) and films containing various quantities (6 %, 9 %, 12 %, and 15 %) of SFW. Within the control film, microscopic particles aggregated during film dehydration as a result of differing rates of heat transfer in the water evaporator from emulsion components (agar and methylcellulose). The film's top surface was exposed to air drying and quickly lost water in compared to the bottom of the film during solidification, which is related to differences in the biomaterials' physical and chemical structures (Kowalczyk & Baraniak, 2014). This is especially true of methylcellulose, which has highly intensive crystallinity, as expressed in the XRD pattern. The film involved various SFW percentages; the naked formation of globules aggregates of wax may be related to a higher melting point temperature (74–80 °C) than the film drying (30–35 °C) (Goslinska & Heinrich, 2019; Syahida et al., 2020). A few spots in film scanning may also occur, resulting in decreased contact between non-polar SFW globules and polar molecules (agar and methylcellulose). This could be related to increased wax percentages, causing a rise in wax globule size on the film surface (Kowalczyk & Baraniak, 2014; Syahida et al., 2020), or tiny air bubbles forming during casting, which leaves spots after the film dehydrations. Furthermore, previous studies (Alizadeh-Sani et al., 2021; Hashim et al., 2022) found that the film surface could be smoother by incorporating anthocyanins, making them an ideal candidate for comparison with a film containing waxes without anthocyanins (Kowalczyk & Baraniak, 2014; Syahida et al., 2020).

4.3.3. X-ray diffraction spectra

The XRD diffraction spectra studies of the crystalline construction features of diverse SFW, methylcellulose, agar, and colorimetric films are shown in Fig.S.3. The SFW powder diffractogram revealed two distinct sharp peaks at 21.5° and 23.9° with a crystalline structure similar to most natural waxes such as sugarcane wax, bee wax, and carnauba wax (20–25°) (Hashim et al., 2022; York et al., 2019). According to Bäumlner et al. (2013) SFW had long linear molecules of esters fatty acid associated with the ester bond (66–69 %, C₃₈–C₅₂), which

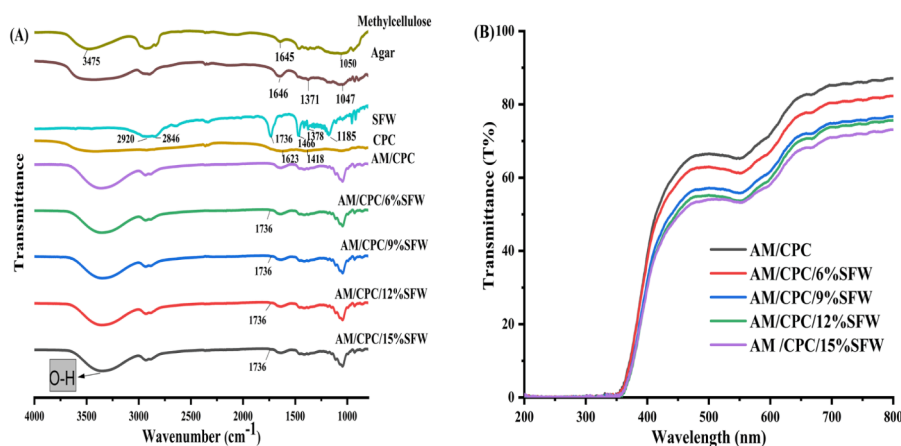


Fig. 2. (A) FTIR of Agar, Methylcellulose, CPC, SFW and colorimetric film with SFW contents at 0%,6%, 9 %, 12 % and 15 % (B) Light transmission of the various colorimetric films in the ultraviolet (UV) light (200–320 nm) and visible light (400–800 nm).

could provide a strong correlation through end groups of alkane and along with the theoretical Van der Waals forces (Doan et al., 2017). Agar powder showed 13.2° and 19.8° broadband diffraction peaks associated with the second crystalline structure of a co-polymer of galactose and 3,6 anhydrogalactose (Kumar et al., 2019).

The peaks at 8.5° and 20.1° confirm the existence of methylcellulose crystallinity as a result of strong internal and external bonding due to hydrogen bonds (Kelnar et al., 2020). It was observed that the control film's spectra (AM/CPC) were observed in the three broad peaks at 19.8°, 12.9°, and 7.5°, which differed from the spectra of film-forming materials, indicating the agar and the methylcellulose fusions in the films. The peak shift at 7.5° which represented the methylcellulose, while 19.8° and 12.9° represented the agar.

Furthermore, the increased intensity of the AM/CPC composite broad peak at ~21° could correlate with increased SFW in the film, representing the lipid's crystallinity reflection. This indicates SFW's ability for miscibility and compatibility with biomaterials inter films containing hydrogen bonds and forming film networks (Huang et al., 2019). Therefore, the XRD results demonstrate that the smart film's biomaterial components are well-distributed.

4.4. Mechanical properties

Table 1 shows the thickness (μm), tensile strength (TS, MPa), and elongation at break (EB, %) of the colorimetric films. The increase in the SFW concentrations increased the thickness of the films considerably ($P < 0.05$) from 170 to 200 μm . In the same way, in previous studies, adding sugarcane wax to agar and palm wax with gelatin in different amounts made the film thicker (Hashim et al., 2022; Syahida et al., 2020).

The increase in the SFW concentrations improved the TS and EB, which are indicators of tolerance performance during production and handling. In addition, AM/CPC/15 %SFW had the best force endurance among the films. This could have been caused by the biomaterial's highly ordered polymer structure. In the same trend, TS and EB were

Table 1
Physical and mechanical properties of the colorimetric films.

Physical properties	Film types				
	AM/CPC	AM/CPC/6% SFW	AM/CPC/9% SFW	AM/CPC/12 %SFW	AM/CPC/15 %SFW
Moisture content (%)	4.945 \pm 0.004 ^a	3.749 \pm 0.003 ^b	2.685 \pm 0.001 ^c	2.389 \pm 0.001 ^d	2.113 \pm 0.001 ^e
Water solubility (%)	43.829 \pm 0.000 ^a	39.668 \pm 0.000 ^b	34.579 \pm 0.002 ^c	34.288 \pm 0.000 ^{cd}	33.858 \pm 0.001 ^d
Swelling capacity (%)	69.711 \pm 0.001 ^a	50.387 \pm 0.008 ^{ab}	45.938 \pm 0.000 ^b	44.390 \pm 0.027 ^b	35.540 \pm 0.027 ^c
WVP (g.mm ⁻² .d ⁻¹ .pa ⁻¹) $\times 10^7$	2.230 \pm 0.000 ^b	2.180 \pm 0.000 ^d	2.150 \pm 0.000 ^e	2.200 \pm 0.006 ^c	2.250 \pm 0.000 ^a
Mechanical properties					
Thickness (μm)	170.330 \pm 0.001 ^a	182.667 \pm 0.001 ^c	184.217 \pm 0.001 ^c	191.667 \pm 0.001 ^b	200.167 \pm 0.001 ^d
Tensile strength (MPa)	1.569 \pm 0.007 ^c	1.795 \pm 0.007 ^d	1.979 \pm 0.003 ^c	2.267 \pm 0.044 ^b	2.799 \pm 0.025 ^a
Elongation at break (%)	87.590 \pm 1.259 ^e	93.305 \pm 0.530 ^d	124.690 \pm 1.004 ^c	132.800 \pm 0.495 ^b	145.875 \pm 1.379 ^a
Optical properties					
Transparency (%)	10.900 \pm 0.000 ^a	9.982 \pm 0.000 ^b	9.714 \pm 0.000 ^c	9.254 \pm 0.000 ^d	8.816 \pm 0.000 ^e
Opacity	422.200 \pm 0.000 ^a	366.700 \pm 0.000 ^b	334.800 \pm 0.000 ^c	311.500 \pm 0.000 ^d	290.700 \pm 0.000 ^e

Values are given as mean \pm standard deviation. Different superscript letters indicate that the means are significant ($p < 0.05$).

increased when palm wax was added to gelatin film (Syahida et al., 2020). Zhang et al. (2018) had similar findings when comparing beeswax and carnauba wax in gelatin film and discovered that bee wax had the greatest TS and EB due to its soft and viscous texture, which contributed to the structure of the film. The results showed that including SFW on colorimetric films could improve the mechanical properties of food packages.

4.5. Moisture barrier properties of the colorimetric films

4.5.1. MC, WS, and S of the colorimetric films

MC, WS, and S are crucial parameters for the permeability of biomaterials used in packaging films, mainly containing anthocyanin dyes with high hydrophilicity affecting packaging applications (Dong et al., 2020). Increased SFW concentration resulted in a significant difference ($P < 0.05$) in Table 1. The hydrophilicity of the natural dyes (CPC) and AM demonstrated a substantial degree of water affinity when AM/CPC was used as a control film. Notably, the resistance to moisture of the films increased in percentage with rising amounts of SFW. This could be attributed to the number of long-chain fatty acid alcohol and alkanes, which made the films more hydrophobic, thereby reducing the binding side connected with water (Zhang et al., 2018). Nonetheless, there were no significant differences ($P > 0.05$) in S% between the AM/CPC/9% SFW and AM/CPC/12 %SFW films. According to previous research (Kowalczyk & Baraniak, 2014), this indicates the presence of an aperture or cracks in the film matrix.

Previous studies observed that incorporating various types of wax (bee wax, carnauba wax, palm wax and sugarcane wax) into film materials enhanced the ability to reduce moisture content (Cortés-Rodríguez et al., 2020; Hashim et al., 2022; Syahida et al., 2020). Therefore, reducing MC, WS, and S is preferable to the water resistance in the colorimetric packages.

4.5.2. WVP of the colorimetric films

WVP is essential for measuring the exchange of moisture vapor between food packaging film and the environment to maintain food product shelf-life. The WVP was decreased significantly ($P < 0.05$) until 12 % SFW than control film (AM/CPC) and then retrogradation with an increased composition of SFW (15 %). That means the rise in WVP indicates that the film composition of lipid material above certain levels is influenced by water vapor diffusion and the presence of cracks and tiny holes (Kowalczyk & Baraniak, 2014; Syahida et al., 2020). In compared with colorimetric films utilizing various SFW ratios, 9 % was the optimum ratio for reducing WVP. This optimum reduction of WVP of SFW (9 %) conflicted with palm wax, which was 15 % (Syahida et al., 2020). A previous study by Y. Zhang et al. (2018) revealed differences between beeswax and carnauba wax when added to gelatin film at the same percentage, resulting in a high-density structure of saturated fats and a comprehensive study of long fatty acid chain alkanes and alcohols with the ability to reduce WVP. These attributes of the SFW phenomena were confirmed by an XRD analysis films', indicating that the SFW exhibited high fatty acid crystallinity and a long fatty acid chain (Baümler et al., 2013). As a result, SFW films were given more control to reduce WVP.

4.6. Anthocyanin release from the colorimetric films

A release analysis was done to determine the ability of AM and SFW to protect the CPC anthocyanin dye. The rate of CPC dye leached from the colorimetric film was observed in Fig.S.4. A maximum absorbance of 0.695 by the CPC solution was revealed at 546 nm, compared with AM/CPC, AM/CPC/6%SFW, AM/CPC/9%SFW, AM/CPC/12 %SFW, and AM/CPC/15 %SFW. These were released at 0.021, 0.016, 0.014, 0.012, and 0.005, respectively after immersion of the film for 10 h in 50 % simulant, except for the AM/CPC release 0.001 in 95 % of the simulant and other films remained colorless after 10 h. Thus, the rate of anthocyanin release from the colorimetric film matrix was determined by the

biopolymer solubility and polarity of the film and food simulants. It was further observed that when SFW amounts (hydrophobic, non-polar) were increased, the film exhibited greater non-polarity, thereby restricting the CPC anthocyanin release from the film matrix, which concurs with observations made in previous studies (Alizadeh et al., 2021; Liang et al., 2019).

4.7. Light barrier property of films

The light barrier is an important parameter that needs more concern in processed food packaging, especially ones containing natural pigments (anthocyanins) that are more sensitive to deterioration by ultraviolet light. Therefore, it is appropriate to protect foods containing nutrients such as vitamins from the amount of light. It is interesting to note that all films showed a vital capability to protect against the UV region (320) to zero, as shown in Fig. 2B.

When compared with the AM/CPC control ($\lambda \leq 350$), the addition of SFW (6 %, 9 %, 12 %, and 15 %) was maximized and defened approximately in AM/CPC/6%SFW ($\lambda \leq 355$), AM/CPC/9%SFW ($\lambda \leq 358$), AM/CPC/12 %SFW ($\lambda \leq 359$), and AM/CPC/15 %SFW ($\lambda \leq 361$).

This could correlate to SFW content being pale yellow plus surfactant emulsion soy lecithin, and tween80 has brownish-yellow may also promote and improve UV region in SFW films, which was similar to reported studies (Dos Santos et al., 2017; Hashim et al., 2022; Syahida et al., 2020). Moreover, all films with integrated SFW percentages showed stronger protection transmission ($P < 0.05$) in visible light range of 400–800 nm from AM/CPC (88 %) to 82 %,77 %,75 %, and 73 % respectively. Perhaps films containing wax distribution particles were opaque and thus more able to reduce light dispersing influence on the films. This is consistent with studies concerning various types of natural waxes (Dos Santos et al., 2017; Hashim et al., 2022; Syahida et al., 2020). Additionally, anthocyanin can visibly absorb and UV light, as previously reported by Alizadeh et al. (2021). Consequently, the transparency and opacity of the colorimetric film were calculated at 600 nm wavelength in Table.1. Noticeably, increased SFW percentages in colorimetric films acted as stronger light barriers, which reduced overall transparency and opacity.

4.8. Thermal stability of colorimetric films

Thermogravimetric analysis (TGA) and differential thermogravimetric (DTG) are important food packaging analyses used to detect packaging ability to heat resistance by measuring the changes in weight film during exposure to various temperature ranges. The thermal analysis determined the SFW films of TGA and DTG profiles as shown in Fig. 3.

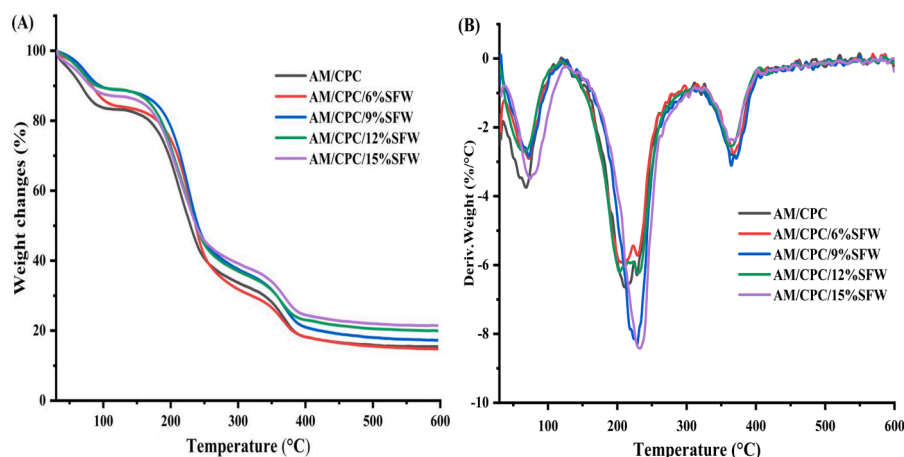


Fig. 3. (A) TGA (B) DTG profiles of colorimetric films.

The TGA profile offers the mass of the film contrasted with temperature throughout the heating process, while the DTG represents the rate of weight change ($\Delta W/\Delta T$) against temperature. The TGA spectra displayed a similar overlapping trend to the film's thermal disintegration, involving three prominent thermal zones of weight loss during heating. The first thermal zone occurred at 46.5 °C–99 °C with a minor mass loss of (1.06 %–8%) moisture content. The second thermal cycle obtained at around 177.5 °C–252.7 °C is the most prominent since the maximum mass loss (34.8 %–37.7 %) was caused by glycerol decomposition. The third thermal zone happened at approximately 343.7 °C–393 °C, although (AM/CPC) correspondence with (AM/CPC/6%SFW) experienced with mass loss of (6.5 %–9.5 %) after the final thermal decomposition of films with a higher proportion of residue mass (14.72 %–21.4 %) occurring at 599 °C. Furthermore, as the SFW percentage increased, the DTG profiles shifted from sharp to board peaks, resulting in a maximum thermal decomposition rate of 228 °C to 234 °C; this is suggested by the complexity of the film polymer material and with desired parameters of the food packaging material for heat resist degradation in the typical temperature range of 150 °C–200 °C (Narasagoudr et al., 2021). Similar results were previously achieved in various biopolymers when using anthocyanins (Alizadeh-Sani et al., 2021; Alizadeh et al., 2021) and natural wax (Liu et al., 2021; Wang & Zhao, 2021).

4.9. Antioxidant activity of films

Intelligent food packaging materials with radical scavenging play an essential role in protecting foods from damage and oxidative degradation. Previous studies confirm that smart packaging films could increase the antioxidant ability of biopolymer films' (Alizadeh et al., 2021; Wu et al., 2021). Anthocyanins are considered to be sources of antioxidant components (Wu et al., 2021). The antioxidant activities within CPC anthocyanins films are illustrated in Fig.S5. The colorimetric films exhibited a significant antioxidant reduction ($P < 0.05$) with increased SFW percentages. When CPC anthocyanin dyes are loaded into the film material, they may be affected by heating and mechanical processing during the process film-forming and reduction. Thus, these outcomes demonstrate that CPC could be potentially utilized as a natural antioxidant for active packaging.

4.10. Color stability of colorimetric films

Color stability is a major parameter for evaluating the color found in smart packaging performance regarding freshness. The color variation (ΔE) values of CPC anthocyanin films remained at 4 °C and 25 °C for up to 16 days as shown in Fig.S.6. Evidently, colorimetric films stored at

4 °C have a small ΔE value for up to 10 days, after which it rapidly increases to 4.7 at 16 days, in comparison with the film held at 25 °C, which had an ΔE value of 3.7 at 10 days and 5.3 subsequently at the end of storage. The AM/CPC indicator revealed a well-formed color stability ΔE value at two storage temperatures. Other films were closed ΔE value which consistently increased per day at 4 °C. However, when 25 °C was reached, these ΔE values were gradually raised at contrasting levels. The color stability variation in ΔE values of the film was affected by a noticeable increase in SFW percentages compared with the constant ratio of CPC anthocyanin. Color stability was proportionately reduced and reminded consistent across the RACN ranges (Zhai et al., 2017). Furthermore, the porous film may have allowed more oxidation, moisture, and temperature to reduce color despite the variable sample (J. Zhang et al., 2019, 2021). However, ΔE values indicate a good color stability within films stored at 4 °C and 25 °C storage.

4.11. The sensitivity of films to pH and ammonia solution

The pH sensitivity of the films is shown in Fig. 4a. When the pH was elevated, the colorimetric films changed from red-pinkish hue to bluish green; it is clear that the color reaction to the pH change of the colorimetric films differed slightly from the CPC solution. This suggests that

CPC interacts with other biomaterial components (containing AM and various SFW percentages), which also possessed certain colors characteristics (Dos Santos et al., 2017; Hashim et al., 2022; Syahida et al., 2020). Thus, it could confirm further structural transformations of color by increasing pH levels. In highly acidic pH solutions of (2 and 3), all films appeared flavylum cation (red) and purple when acidity was reduced to (4 and 5). In neutral pH solutions of 6 and 7, the films showed pink color. Conversely, increased pH alkalinity values of (8–11) shifted from pale green to a darker variant of green. Notably, the high base pH (12) dominated the quinoidal base and transformed the color to a bluish-green hue. Our results suggest that the developed colorimetric films can function well as pH indicators to monitor food freshness.

Volatile nitrogen compounds are regularly produced from contaminants rich animal protein by microorganisms as an indicator of spoilage. Ammonia vapor, as one such generated compound, was employed to simulate food deterioration and convert the package environment to alkalinity, a sign of spoiled animal foodstuffs. Previous studies confirmed ammonia's ability to appear different colors when reacting with anthocyanin in colorimetric films according to concentration, time duration, and the moisture content process (Alizadeh et al., 2021; Wu et al., 2021). The CPC's test sensitivity (S_{RGB}) in colorimetric films was attributed towards the volatile basic gas exposure in a (100 mmol/L)

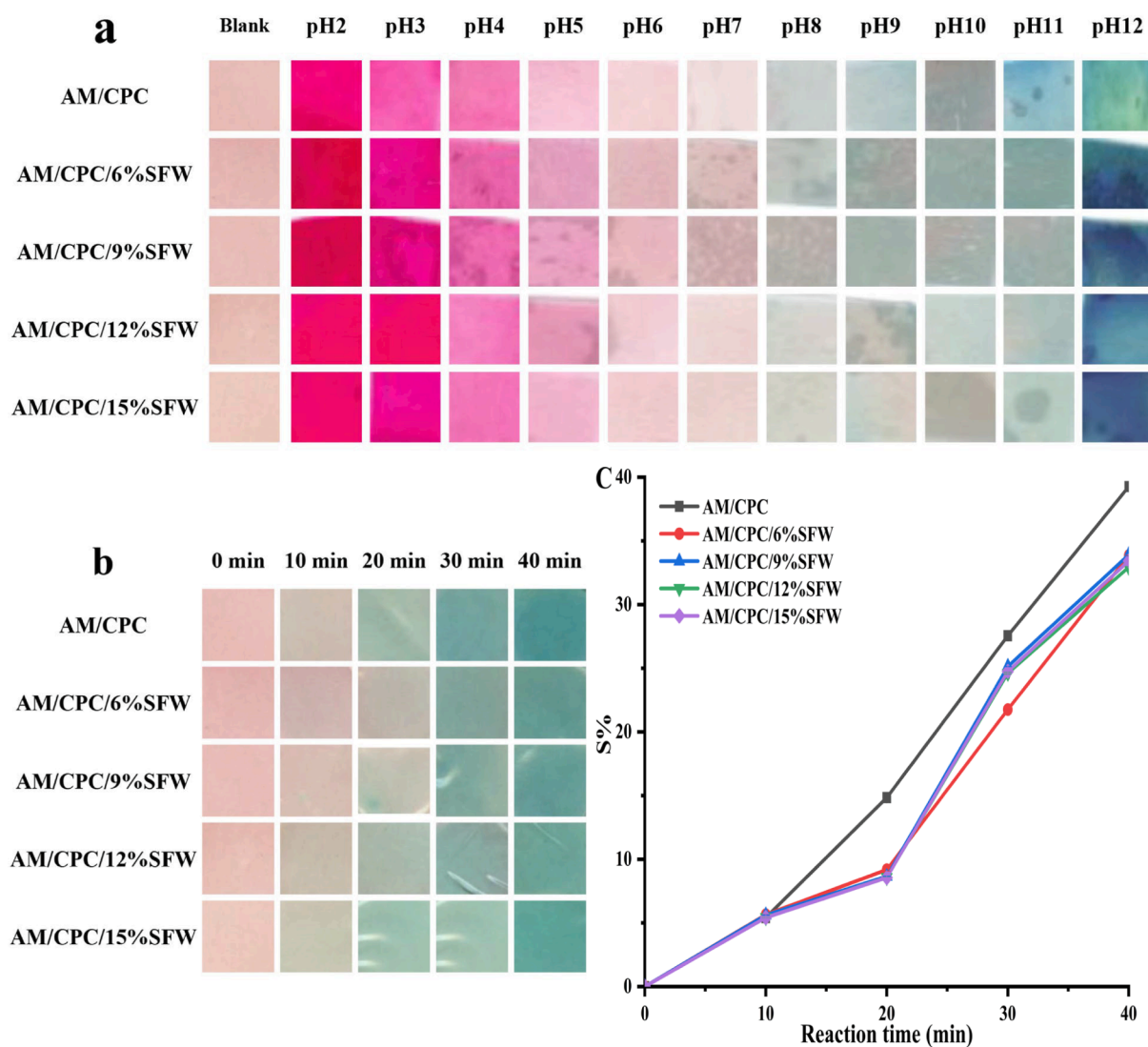


Fig. 4. (a) Visual color of colorimetric films response to pH 2.0–12.0; (b) response to ammonia gas at 100 mmol/L; (c) sensitivity (%).

ammonia solution under room temperature for 40 min. The colorimetric films changed from pink to dark green after 40 min of exposure in response to the ammonia vapor. The color variations of films and sensitivity to ammonia vapor are shown in Fig. 4b, c.

Over time, the indicator (S_{RGB}) increased by approximately 5 % after 10 min in all films. The control film AM/CPC offered the highest sensitivity of nearly 14.8 %, 27.6 %, and 39.3 % at 20, 30, and 40 min. The film's material components (AM and CPC) were hydrophilic due to fast saturation with ammonia resulting in a color change. However, other films attributed the similar results with a slight (S_{RGB}) color change after 10 min; this proved to be more significant than the 9.2 % contained in AM/CPC/6%SFW. At 30 min premeditate, AM/CPC/9% SFW has the highest sensitivity at 25 %, with similar color-changes at 24 % in AM/CPC/12 %SFW and AM/CPC/15 %SFW, and AM/CPC/6%SFW reaching at least 21.8 %. The apparent color change and high sensitivity after saturation with ammonia vapor produced a modest sensitivity variation of roughly 33 %. Ammonia was used to react with several colorimetric films containing various SFW percentages, leading to enhanced penetration and color transformations (Hashim et al., 2022). The film designed as a smart sensing indicator was approved for work as a colorimetric biomarker film.

4.12. The application for monitoring chicken breast spoilage

As shown in Fig. 5, all colorimetric films can be used as a non-destructive assessment of TVB-N and ΔE values, a freshness/spoilage indicator for chicken breast, by altering the color within the storage time (approximately 42 h at 25 °C).

TVB-N was detected and produced during chicken meat spoilage, making it possible to identify the overall freshness/spoilage rate of chicken meat. This study proved that the films could detect volatile nitrogen compounds when their colors changed due to exposure from these compounds. According to color changes (ΔE values) in films at 27 h, the films were arranged according to their ability to detect nitrogen compounds as follows: AM/CPC > AM/CPC/9%SFW > AM/CPC/12 % SFW > AM /CPC/15 %SFW > AM/CPC/6%SFW. The initial level of chicken freshness was 8.8 mg/100 g (pink color), then increased to 20.6 mg/100 g at 18 h (dark pink) and 26.3 mg/100 g at 27 h (green color) as the quality deteriorated. These results were within the limit specified by scientific studies (25–28 mg/100 g) for the starting point of chicken meat spoilage, and this level was derived from the total viable count and sensory attributes (Farahnaz et al., 2016; Senapati & Sahu, 2020). In addition, chicken spoilage storage time was agreement with that obtained by Othman et al. (2018). Freshness indicator films showed a strong positive correlation between TVB-N contents and ΔE ($R < 0.90$)

(Table S.2), as there was a noticeable change during and after passing the limit of acceptance.

4.13. Selection of best film

There have been major breakthroughs in smart packaging by creating packages made with natural biopolymer materials (matrix) and integrated with sensitive colorimetric compounds (known as natural pigments). There are two key aspects for evaluating the quality of pH colorimetric packaging: The main aspect is the water vapor permeability (WVP) which indicates the package's ability to prevent the permeability of water vapor and exposure to environmental elements, thus protecting the packaging and food from deterioration. A good WVP rate indicates that the film matrix is free of fractures and pinholes as a result of good quantity/distribution of the film's biomaterial. Based on these findings, the AM/CPC/9%SFW film was considered the best out of all the tested films (Kowalczyk & Baraniak, 2014; Syahida et al., 2020). The other aspect is sensitivity of pigments in the film detected the ammonia vapor resulting from food spoilage (Zhai et al., 2017; Zhao et al., 2022). As such, the AM/CPC/9%SFW film demonstrated the best color change abilities due to its highest reactions ammonia in the ammonia sensitivity assay and food application.

5. Conclusion

New pH colorimetric smart films that integrate SFW and CPC anthocyanins within AM matrix have been developed as a biomarker of chicken breast freshness. Based on our results, the addition of SFW significantly reduced moisture properties, improved thermal and mechanical capabilities, and considerably enhances the anthocyanin stability emitted into the film. At pH ranges 2–12, it was confirmed CPC color changes from red, purple and yellow. A fundamental change occurred from the introduction of SFW through light transmission, protecting against UV-vis and declining visible light. The films showed apparent color variations in response to varying pH levels and ammonia vapor sensitivity. Finally, our results revealed a positive association between TVB-N and film color changes at real-time identification of fresh food (chicken breast). More notably, the AM/CPC/9%SFW possessed the best WVP ratios, exhibited excellent ammonia vapor sensitivity, and contained a high ΔE value for visible color transformation in response to TVBN. To our knowledge, this is the first application and confirmation of SFW as a natural wax and CPC anthocyanin in the development of intelligent food packaging films. Future research will concentrate on enhancing SFW film with active compounds and exploring the utilization of other natural waxes, particularly

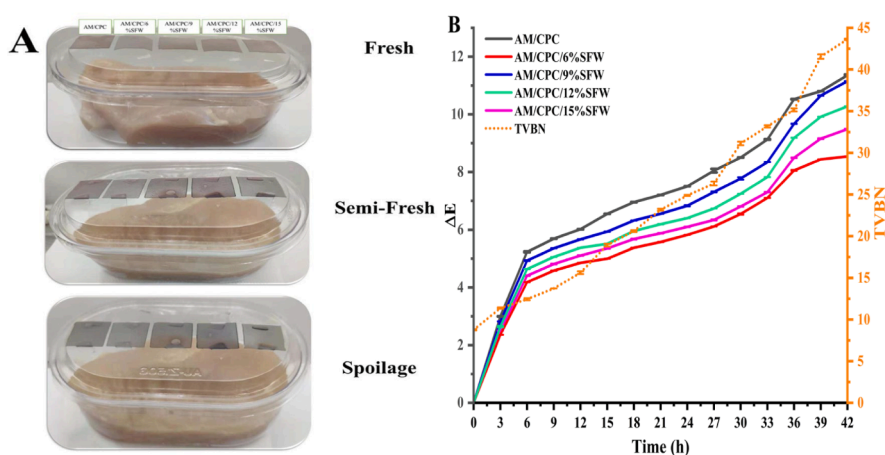


Fig. 5. (A) The corresponding color changes of colorimetric films. (B) the change of TVB- values of chicken breast and ΔE of indicator films stored at 25 °C and the corresponding color changes of colorimetric films.

by-products of the food industry, as biosensors in smart food packaging systems.

CRedit authorship contribution statement

Sulafa B.H. Hashim: Data curation, Writing – original draft. **Haroon Elrasheid Tahir:** Writing – review & editing. **Li Lui:** Conceptualization, Methodology. **Junjun Zhang:** Writing – review & editing. **Xiaodong Zhai:** Writing – review & editing. **Amer Ali Mahdi:** Writing – review & editing. **Nosyba A. Ibrahim:** Writing – original draft. **Gustav Komla Mahunu:** Writing – review & editing. **Mahmoud M. Hassan:** Conceptualization, Methodology. **Zou Xiaobo:** Conceptualization, Methodology. **Shi Jiyong:** Conceptualization, Methodology.

Declaration of Competing Interest

The authors declare that they have no known competing financial interests or personal relationships that could have appeared to influence the work reported in this paper.

Data availability

No data was used for the research described in the article.

Acknowledgments

This work was supported by the National Natural Science Foundation of China [grant numbers 31772073, 31671844]; and Priority Academic Program Development of Jiangsu Higher Education Institutions (PAPD).

Appendix A. Supplementary data

Supplementary data to this article can be found online at <https://doi.org/10.1016/j.foodchem.2022.133824>.

References

- Alizadeh-Sani, M., Tavassoli, M., Mohammadian, E., Ehsani, A., Khaniki, G. J., Priyadarshi, R., & Rhim, J. W. (2021). pH-responsive color indicator films based on methylcellulose/chitosan nanofiber and barberry anthocyanins for real-time monitoring of meat freshness. *International Journal of Biological Macromolecules*, *166*, 741–750. <https://doi.org/10.1016/j.ijbiomac.2020.10.231>
- Alizadeh, M., Tavassoli, M., Hamishehkar, H., & Julian, D. (2021). Carbohydrate-based films containing pH-sensitive red barberry anthocyanins: Application as biodegradable smart food packaging materials. *Carbohydrate Polymers*, *255* (November 2020), 117488. <https://doi.org/10.1016/j.carbpol.2020.117488>.
- Azarifar, M., Ghanbarzadeh, B., Sowti khiabani, M., Akhondzadeh basti, A., & Abdulkhani, A. (2020). The effects of gelatin-CMC films incorporated with chitin nanofiber and Trachyspermum ammi essential oil on the shelf life characteristics of refrigerated raw beef. *International Journal of Food Microbiology*, *318*(December 2019), 10.1016/j.ijfoodmicro.2019.108493.
- Bäumler, E. R., Carelli, A. A., & Martini, S. (2013). Physical properties of aqueous solutions of pectin containing sunflower wax. *JAOCs, Journal of the American Oil Chemists' Society*, *90*(6), 791–802. <https://doi.org/10.1007/s11746-013-2235-y>
- Bhargava, N., Sharanagat, V. S., Mor, R. S., & Kumar, K. (2020). Active and intelligent biodegradable packaging films using food and food waste-derived bioactive compounds: A review. *Trends in Food Science and Technology*, *105*, 385–401. <https://doi.org/10.1016/j.tifs.2020.09.015>
- Cortés-Rodríguez, M., Villegas-Yépez, C., Gil González, J. H., Rodríguez, P. E., & Ortega-Toro, R. (2020). Development and evaluation of edible films based on cassava starch, whey protein, and bees wax. *Heliyon*, *6*(9). <https://doi.org/10.1016/j.heliyon.2020.e04884>
- Doan, C. D., To, C. M., De Vrieze, M., Lynen, F., Danthine, S., Brown, A., ... Patel, A. R. (2017). Chemical profiling of the major components in natural waxes to elucidate their role in liquid oil structuring. *Food Chemistry*, *214*, 717–725. <https://doi.org/10.1016/j.foodchem.2016.07.123>
- Dong, H., Ling, Z., Zhang, X., Zhang, X., Ramaswamy, S., & Xu, F. (2020). Smart colorimetric sensing films with high mechanical strength and hydrophobic properties for visual monitoring of shrimp and pork freshness. *Sensors and Actuators, B: Chemical*, *309*(January), Article 127752. <https://doi.org/10.1016/j.snb.2020.127752>
- Dos Santos, F. K. G., De Oliveira Silva, K. N., Xavier, T. D. N., De Lima Leite, R. H., & Aroucha, E. M. M. (2017). Effect of the addition of carnauba wax on physicochemical properties of Chitosan films. *Materials Research*, *20*, 485–491. <https://doi.org/10.1590/1980-5373-mr-2016-1010>
- Farahnaz, G.-M., Reza Housaindokht, M., Mohsenzadeh, M., & Varidi, M. (2016). Microbial and chemical spoilage of chicken meat during storage at isothermal and fluctuation temperature under aerobic conditions. *Iranian Journal of Veterinary Science and Technology*, *8*(1), 38–46. <https://doi.org/10.22067/veterinary.v8i1.54563>
- Goslinska, M., & Heinrich, S. (2019). Characterization of waxes as possible coating material for organic aerogels. *Powder Technology*, *357*, 223–231. <https://doi.org/10.1016/j.powtec.2019.08.096>
- Halim, A. L. A., Kamari, A., & Phillip, E. (2018). Chitosan, gelatin and methylcellulose films incorporated with tannic acid for food packaging. *International Journal of Biological Macromolecules*, *120*, 1119–1126. <https://doi.org/10.1016/j.ijbiomac.2018.08.169>
- Hashim, S. B. H., Elrasheid Tahir, H., Liu, L., Zhang, J., Zhai, X., Ali Mahdi, A., ... Jiyong, S. (2022). Intelligent colorimetric pH sensing packaging films based on sugarcane wax/agar integrated with butterfly pea flower extract for optical tracking of shrimp freshness. *Food Chemistry*, *373*(PB), Article 131514. <https://doi.org/10.1016/j.foodchem.2021.131514>
- He, Q., Zhang, Z., & Zhang, L. (2016). Anthocyanin accumulation, antioxidant ability and stability, and a transcriptional analysis of anthocyanin biosynthesis in purple heading Chinese Cabbage (*Brassica rapa* L. ssp. *pekinensis*). *Journal of Agricultural and Food Chemistry*, *64*(1), 132–145. <https://doi.org/10.1021/acs.jafc.5b04674>
- Huang, S., Xiong, Y., Zou, Y., Dong, Q., Ding, F., Liu, X., & Li, H. (2019). A novel colorimetric indicator based on agar incorporated with *Arnebium* euchroma root extracts for monitoring fish freshness. *Food Hydrocolloids*, *90*, 198–205. <https://doi.org/10.1016/j.foodhyd.2018.12.009>
- Kalpna, S., Priyadarshini, S. R., Maria Leena, M., Moses, J. A., & Anandharamkrishnan, C. (2019). Intelligent packaging: Trends and applications in food systems. *Trends in Food Science and Technology*, *93*(October 2018), 145–157. <https://doi.org/10.1016/j.tifs.2019.09.008>
- Kanatt, S. R. (2020). Development of active/intelligent food packaging film containing *Amaranthus* leaf extract for shelf life extension of chicken/fish during chilled storage. *Food Packaging and Shelf Life*, *24*(February 2019), 100506. <https://doi.org/10.1016/j.fpsl.2020.100506>
- Kelnar, I., Zhigunov, A., Kaprálková, L., Krejčíková, S., & Dybal, J. (2020). Synergistic effects in Methylcellulose/Hydroxyethylcellulose blend: Influence of components ratio and graphene oxide. *Carbohydrate Polymers*, *236*(February). <https://doi.org/10.1016/j.carbpol.2020.116077>
- Khoo, H. E., Azlan, A., Tang, S. T., & Lim, S. M. (2017). Anthocyanidins and anthocyanins: Colored pigments as food, pharmaceutical ingredients, and the potential health benefits. *Food and Nutrition Research*, *61*(1). <https://doi.org/10.1080/16546628.2017.1361779>
- Kowalczyk, D., & Baraniak, B. (2020). Effect of candelilla wax on functional properties of biopolymer emulsion films - A comparative study. *Food Hydrocolloids*, *41*, 195–209. <https://doi.org/10.1016/j.foodhyd.2014.04.004>
- Kumar, S., Chandra, J., Ray, D., Mukherjee, A., & Dutta, J. (2019). Heliyon Bionanocomposite films of agar incorporated with ZnO nanoparticles as an active packaging material for shelf life extension of green grape. *Heliyon*, *5*(May), e01867.
- Liang, T., Sun, G., Cao, L., Li, J., & Wang, L. (2019). A pH and NH₃ sensing intelligent film based on *Artemisia sphaerocephala* Krasch. gum and red cabbage anthocyanins anchored by carboxymethyl cellulose sodium added as a host complex. *Food Hydrocolloids*, *87*, 858–868. <https://doi.org/10.1016/j.foodhyd.2018.08.028>
- Liu, C., Zheng, Z., Xi, C., & Liu, Y. (2021). Journal of Colloid and Interface Science Exploration of the natural waxes-tuned crystallization behavior, droplet shape and rheology properties of O / W emulsions. *Journal of Colloid and Interface Science*, *587*, 417–428. <https://doi.org/10.1016/j.jcis.2020.12.024>
- Mostafaei, F. S., & Zaeim, D. (2020). Agar-based edible films for food packaging applications - A review. *International Journal of Biological Macromolecules*, *159*, 1165–1176. <https://doi.org/10.1016/j.ijbiomac.2020.05.123>
- Narasagoudar, S. S., Shanbhag, Y., Chougale, R. B., Baraker, B. M., Masti, S. P., & Lobo, B. (2021). Thermal degradation kinetics of ethyl vanillin crosslinked chitosan / poly (vinyl alcohol) blend films for food packaging applications. *Chemical Data Collections*, *34*(October 2020), 100739. <https://doi.org/10.1016/j.cdc.2021.100739>
- Nasatto, P. L., Pignon, F., Silveira, J. L. M., Duarte, M. E. R., Nosedá, M. D., & Rinaudo, M. (2015). Methylcellulose, a cellulose derivative with original physical properties and extended applications. *Polymers*, *7*(5), 777–803. <https://doi.org/10.3390/polym7050777>
- Oliveira Filho, J. G. de, Braga, A. R. C., Oliveira, B. R. de, Gomes, F. P., Moreira, V. L., Pereira, V. A. C., & Egea, M. B. (2021). The potential of anthocyanins in smart, active, and bioactive eco-friendly polymer-based films: A review. *Food Research International*, *142*(October 2020), 110202. <https://doi.org/10.1016/j.foodres.2021.110202>
- Othman, M., Yusup, A. A., Zakaria, N., & Khalid, K. (2018). Bio-polymer chitosan and corn starch with extract of *hibiscus rosa-sinensis* (hibiscus) as pH indicator for visually-smart food packaging. *AIP Conference Proceedings*, *1985*. <https://doi.org/10.1063/1.5047198>
- Roy, S., Kim, H. J., & Rhim, J. W. (2021). Effect of blended colorants of anthocyanin and shikonin on carboxymethyl cellulose/agar-based smart packaging film. *International Journal of Biological Macromolecules*, *183*, 305–315. <https://doi.org/10.1016/j.ijbiomac.2021.04.162>
- Senapati, M., & Sahu, P. P. (2020). Meat quality assessment using Au patch electrode Ag-SnO₂/SiO₂/Si MIS capacitive gas sensor at room temperature. *Food Chemistry*, *324* (April), Article 126893. <https://doi.org/10.1016/j.foodchem.2020.126893>
- Syahida, N., Pitry, I., Zuriyati, A., & Hanani, N. (2020). Effects of palm wax on the physical, mechanical and water barrier properties of fish gelatin films for food packaging application. *Food Packaging and Shelf Life*, *23*(November 2019), 100437. <https://doi.org/10.1016/j.fpsl.2019.100437>

- Wang, T., & Zhao, Y. (2021). Fabrication of thermally and mechanically stable superhydrophobic coatings for cellulose-based substrates with natural and edible ingredients for food applications. *Food Hydrocolloids*, 120(April), Article 106877. <https://doi.org/10.1016/j.foodhyd.2021.106877>
- Wu, L. T., Tsai, I. L., Ho, Y. C., Hang, Y. H., Lin, C., Tsai, M. L., & Mi, F. L. (2021). Active and intelligent gellan gum-based packaging films for controlling anthocyanins release and monitoring food freshness. *Carbohydrate Polymers*, 254(November 2020), 117410. 10.1016/j.carbpol.2020.117410.
- Yilmaz, E., Uslu, E. K., & Oz, C. (2021). Oleogels of some plant waxes characterization and comparison with sun flower wax oleogel.pdf. *Journal of the American Oil Chemists' Society (JAOCS)*, 643–655. <https://doi.org/10.1002/aocs.12490>
- York, D. W., Collins, S., & Rantape, M. (2019). Measuring the permeability of thin solid layers of natural waxes. *Journal of Colloid and Interface Science*, 551, 270–282. <https://doi.org/10.1016/j.jcis.2019.03.104>
- Zhai, X., Shi, J., Zou, X., Wang, S., Jiang, C., Zhang, J., ... Holmes, M. (2017). Novel colorimetric films based on starch/polyvinyl alcohol incorporated with roselle anthocyanins for fish freshness monitoring. *Food Hydrocolloids*, 69, 308–317. <https://doi.org/10.1016/j.foodhyd.2017.02.014>
- Zhang, J., Huang, X., Zou, X., Shi, J., Zhai, X., Liu, L., Li, Z., Holmes, M., Gong, Y., Povey, M., & Xiao, J. (2021). A visual indicator based on curcumin with high stability for monitoring the freshness of freshwater shrimp, *Macrobrachium rosenbergii*. *Journal of Food Engineering*, 292(May 2020), 110290. 10.1016/j.jfoodeng.2020.110290.
- Zhang, J., Zou, X., Zhai, X., Huang, X. W., Jiang, C., & Holmes, M. (2019). Preparation of an intelligent pH film based on biodegradable polymers and roselle anthocyanins for monitoring pork freshness. *Food Chemistry*, 272(April 2018), 306–312. 10.1016/j.foodchem.2018.08.041.
- Zhang, Y., Simpson, B. K., & Dumont, M. J. (2018). Effect of beeswax and carnauba wax addition on properties of gelatin films: A comparative study. *Food Bioscience*, 26 (October), 88–95. <https://doi.org/10.1016/j.fbio.2018.09.011>
- Zhao, Y., Du, J., Zhou, H., Zhou, S., Lv, Y., Cheng, Y., Tao, Y., Lu, J., & Wang, H. (2022). Biodegradable intelligent film for food preservation and real-time visual detection of food freshness. *Food Hydrocolloids*, 129(December 2021), 107665. 10.1016/j.foodhyd.2022.107665.